clean technologies

MDPI

Article

Application of Plasma Treatment on Coliform Inactivation, Dehydration Kinetics and Quality Attributes of Powder-Form Nutraceuticals

Majid Soleimani * and Oon-Doo Baik

Department of Chemical and Biological Engineering, University of Saskatchewan, Saskatoon, SK S7N 5A9, Canada; oob411@usask.ca

* Correspondence: mas233@usask.ca or soleyir@yahoo.ca; Tel.: +1-(306)374-3035

Abstract: This study was conducted to determine the performance of atmospheric cold plasma (ACP) on powder-form biological materials including wheat flour (WF) and whey protein isolate (WP). Coliform bacteria inactivation and optimization were performed based on a central composite design with two variables, namely residence time and mass of the sample. The results indicated that both variables had a significant effect on bacterial inactivation with more importance of residence time compared to mass of the substrate. The drying process was conducted for selected conditions including mild, moderate, and extreme conditions. The results indicated that plasma can even be used as a fast and effective tool for drying biological materials. Among all models used in this study, the Henderson–Pabis model was more suitable in predicting the dehydration kinetics of both materials. Drying rate constants obtained using this model indicated that the ratios of residence time over mass of the material did not have a significant impact on this parameter. Analysis of the functional properties revealed that water absorption can be highly (≈70%) enhanced in WF. However, properties such as oil absorption (in WF and WP), protein solubility and emulsifying activity index (EAI), and stability (in WP) were slightly changed by the plasma treatment.

Keywords: plasma treatment; coliform bacteria; drying; kinetics; absorption; quality attributes

check for updates

Academic Editor: Patricia Luis Alconero

Received: 17 September 2024
Revised: 21 October 2024
Accepted: 21 January 2025
Published: 3 March 2025

Citation: Soleimani, M.; Baik, O.-D. Application of Plasma Treatment on Coliform Inactivation, Dehydration Kinetics and Quality Attributes of Powder-Form Nutraceuticals. *Clean Technol.* **2025**, *7*, 19. https://doi.org/10.3390/cleantechnol7010019

Copyright: © 2025 by the authors. Licensee MDPI, Basel, Switzerland. This article is an open access article distributed under the terms and conditions of the Creative Commons Attribution (CC BY) license (https://creativecommons.org/licenses/by/4.0/).

1. Introduction

Practical Applications

Atmospheric cold plasma technology is a process that has been developed for the treatment or processing of materials, biomaterials, hygiene products, and organic tissues, as well as food and bioproducts. Its simplicity and the high performance of its applications compared to other systems of cold plasma and conventional technologies make it promising, especially in the field of food and bioproduct processing. It has been proved that it can be used for microbial inactivation and the modification/improvement of some functional properties. This current study aims to investigate its simultaneous effectiveness on multi-aspect features of powder-form materials, namely bacterial inactivation, dehydration, and the improvement of functional properties.

Thermal processing has been extensively implemented by industries to improve the quality of processed food products and to extend their shelf life commercially by inactivation of microbial species. However, some negative impacts on quality properties, nutritional components, and sensory attributes might result from chemical or biochemical

reactions accelerated at higher temperatures (Awuah et al., 2007; Lou et al., 2022; Allai et al., 2023) [1–3].

Some alternative or eco-friendly techniques have been developed or adapted to be used for food or nutraceutical processing such as atmospheric plasma technology, pulsed electric fields, ultrasound, high hydrostatic pressure, and electromagnetic technologies (Allai et al., 2023; Leong et al., 2024; Maccaferri et al., 2024; Pasdar et al., 2024) [3–6]. Among all, plasma technology is the one with diverse applications in material science and processing, physics and chemistry, medicine, polymers, materials, and food processing. Plasma is considered to be the dominant state of matter in the universe, and it is categorized as the fourth state of matter which is actually an ionized form of a gas. If energy (in heat or electromagnetic form) is added to a solid material, it is converted to liquid. By adding more energy, it is partially or completely ionized to generate a new state of matter which is plasma. The energy for plasma generation can be provided from different sources such as the combustion process, laser radiation, electrical discharges in gases, etc. In other words, ionization of a gas using a proper source of energy would generate plasma that could be cold plasma or thermal plasma (Lopez et al., 2019; Tabares, 2021; Tabares and Junkar, 2021) [7–9].

Thermal plasma can be extremely hot with temperatures of up to several thousand degrees Celsius, with applications in material and chemical processing industries where higher temperature is required. Nonthermal or cold plasma is known by characteristics of a low temperature (25 °C to 100 °C) of heavy species such as natural particles and ions. In cold plasma, a wide variety of species including charged particles, radicals, atoms, and molecules and photons are found but, overall, a small fraction of atoms are ionized. However, in hot plasma, the majority or all of the atoms are ionized. (Ouyang et al., 2018; Tabares, 2021; Tabares and Junkar, 2021) [8–10]. Cold plasma (generated by electromagnetic field generators) with lower temperatures is suitable for processing or modification of heat-sensitive materials such as food and bioorganic substances.

Plasma can be generated in different ways with different characteristics at macro- and microscales. On a macroscopic scale, plasmas are electrically neutral, meaning that the number of positive and negative charges is similar. On the other hand, at the microscopic scale, plasmas are characterized by electron density and electron energy. The electron density may vary between 1 and 10^{25} electron/cm^3. The excited and accelerated electrons in the field can cause ionization of the gas molecules and atoms, releasing more electrons in the system with the potential for gas ionization. As a consequence, excitement of the atoms and molecules in such chain reaction generates new atoms, molecules, and free radicals at high energy levels, alongside positive and negative ions, electrons, free radicals, reactive oxygen and nitrogen (as ozone, single oxygen, atomic oxygen, hydroxyl radical, superoxide, nitrogen dioxide and nitric oxide), and even some radiation such as UV radiation, which is in the form of either antimicrobial or reactive substances (Daeschlein et al., 2010; Pankaj et al., 2018) [11,12]. One of the important factors in plasma generation is the pressure of the system. By increasing the pressure, energy can be easier and more efficiently transferred (through collisions) from electrons to gas species such as gas molecules and ions. For the specific case of atmospheric plasma, no special reaction vessel is required to provide low or high pressure in the system. This makes the process easy to apply and less costly to implement. In terms of application, plasma jets or pencils generated from cold atmospheric plasmas may have a wide range of uses in the medical sector (in situ treatment of live tissues, teeth, skin and wound treatment), aqueous media using plasma–liquid interaction, surface modification, etc., (Wolf, 2012) [13].

Due to the reactivity of the active species and radiations in plasma, it can be used for inactivation of a wide range of microbial species such as bacteria, yeasts, molds, and spores,

which are considered more resistant forms of microorganisms (Klampfl et al., 2012; Tseng et al., 2012) [14,15]. The use of plasma under reduced pressure requires less power and voltage for plasma generation in microbial inactivation process that can be performed in a short period of time. However, the process can be more expensive, requiring vacuum equipment and facilities. Compared with the vacuum system, nonthermal atmospheric plasma can be operated under normal pressure without vacuum facilities, so it is significantly less costly to operate.

Most of the research studies on cold plasma treatment/processing of food or nutraceutical products have focused on surface inactivation of microorganisms and biofilms or fixed-bed/bulk systems. In a study by Deng et al. (2007), *E. coli*-inoculated almonds were treated with cold plasma generated by a dielectric barrier discharge apparatus operating at frequencies of 1.0–2.5 kHz [16]. Lassen et al. (2005) used a radiofrequency (RF) system operating at 13.56 MHz to treat *B. stearothermophilus* spores [17]. Various gas mixtures were prepared with O_2, Ar, CF_4, and H_2 and tested at power levels of 100 W and 400 W. A gas mixture of Ar/H_2 at 5%/95% at 20 Pa gave the best antimicrobial result, with a reduction of 2 log cycles after a 3 min treatment. Han et al. (2016) reported that the mechanism of cell inactivation by ACP could be different in microorganisms such that *E. coli* can be damaged by cell leakage and low-level DNA damage, while *Staphylococcus aureus* inactivation would be caused by intracellular damage [18]. Traba and Liang (2015) performed low-power (80–90 W) ACP inactivation of *S. aureus* biofilms using argon as the active gas and concluded that over 99.9% of the population would be killed within 10 min of exposure [19]. Other than bacterial inactivation, cold plasma technology has also been examined as a pre-treatment to improve the drying performance of food products and seeds. Li et al. (2019) reported an accelerated drying process in corn seed using cold plasma for 50 s at 500 W power [20]. Some other positive influences of plasma pre-treatment on the drying process of mushroom and jujube have also been reported by Shishir et al. (2019) and Bao et al. (2020) [21,22].

Although many studies have been carried out on bacterial inactivation in food and nutraceuticals, no work with significant impact or successful results has been accomplished on wheat flour and whey powder using ACP technology. Furthermore, no work has been reported on direct role of ACP in the dehydration process; the focus of others has been on the application of cold plasma as a pre-treatment method to improve the next process of dehydration. In this study, an efficient method of ACP in a fluidized bed using a low power (30 W) was used to inactivate coliform bacteria in powder-form materials (EF and WP). Also, the drying kinetics and performance of ACP were investigated, combined with evaluations of functional and physical properties.

2. Materials and Methods

Powder-form materials including whey protein (Isonatural^{TM}, Allmax, North York, ON, Canada) and wheat flour (Robinhood, Smucker Foods of Canada Corp, Saskatoon, SK, Canada) were used in this study. Violet red bile agar (VRBA), brilliant green lactose bile broth (BGLB) and MacConkey agar were purchased from Thermo Scientific. Coliform bacteria were isolated from the WF after making a 1:5 to 1:100 (WF to normal saline) suspension. A population of 120 CFU/g was detected in WF powder. In a pour plate method, 1 mL of the diluted sample was transferred to VRBA and MacConkey media followed by incubation at 35 °C for 24 h. The colonies formed on VRBA were selected for verification in BGLB medium for gas production in test tubes. After verification as coliforms, they were transferred to VRBA for cell enrichment in the form of colonies. In trials for the purpose of inoculation of the coliforms, assuming that each colony can contain as high as 10^7–10^8 cells, 10 loopfuls of cells were transferred to 15 g of WP or WF with

adjusted moisture content (at 10 and 16%). Mixing of the colonies with the samples of WP and WF was carried out for 2–3 min using a high-speed pulveriser/grinder ((DR Mills, DM 7441) which was disinfected using hydrogen peroxide and 70% ethyl alcohol sequentially) to enable disintegration of colonies. Thereafter, samples were packed in plastic Ziploc bags and stored in the fridge for 16 h for uniform distribution of moisture in the sample. Uniform distribution of the moisture and coliform bacteria in WF and WP was verified by taking 4 samples for each and testing them using the oven drying method at 103 °C.

The inactivation process of the coliform bacteria was conducted on a vortex vibrator to provide high enough fluidization motion in the particles and homogeneous mixing (Figure 1). The samples of WF (wet WF (WFw) and dry WF (WFd)) or WP (wet WP (WPw) and dry WP (WPd)) were located in a cylindrical tube (volume of 10 mL) with a hole in the middle of the cap to provide a wide enough seat for the tip of the plasma wand (Plasma Etch Inc., Carson City, NV, USA) and a distance of approximately 1 cm between plasma and the sample. The vortex machine provides a fast motion of the particles inside the tube horizontally and vertically to fluidize the particles and provide perfect contact between the particles and the plasma. This fluidization provided a consistent result in plasma processing of the samples in terms of bacterial inactivation, color change, etc. However, using a non-fluidized or packed bed of the powder-form material resulted in nonuniform or inconsistent results in the trials. Therefore, this fluidized system, with better and more uniform exposure of particles to plasma gas, using the vortex machine was preferable for employment in the current study. The plasma wand generated a power of up to 30 W to transform the fed gas into the target plasma gas. The plasma wand used in this study was basically a cylindrical device with a power supply (15 V DC, 30 W) at one end and plasma discharge on the other end through a Teflon housing with a pin-end electrode located in the center of the housing. The gas, which was air in this study, was supplied from the side of the device at a preset flowrate controlled using a flowmeter. Extension of the plasma was 5–10 mm with and an effective width of 5–20 mm, which was considered in the design of the treatment setup. A central composite design (with two variables, namely residence time and sample mass) was employed to conduct the plasma treatment. The range of the sample weight was from 0.5 to 1.5 g and the residence time for the treatment was from 5 to 15 min (Table 1). At the end of each treatment, 0.45 g of the sample was used to determine the bacterial load of the treated sample in triplicate. Dilutions of up to 10^7 in normal saline were prepared to determine the CFU of the coliforms.

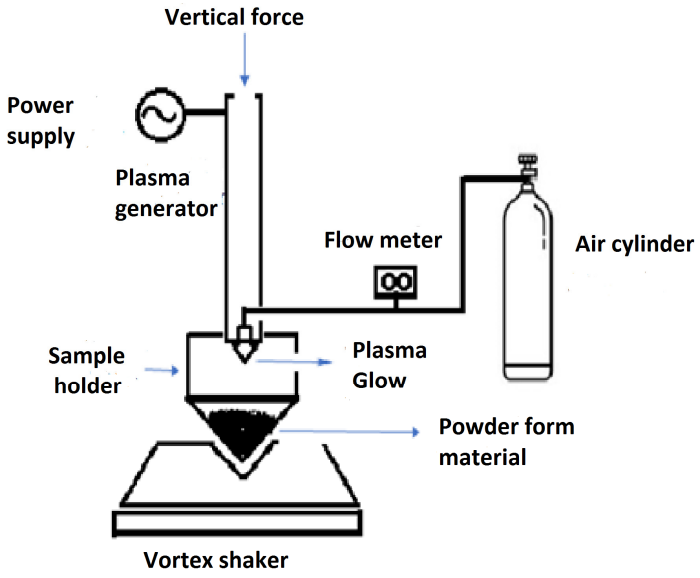

Figure 1. The setup prepared for plasma treatment of the powder-form samples.

Table 1. Experimental central composite design for plasma treatment.

Independent Variable		Levels of the Independent Variables		
	Symbol	**−1**	**0**	**+1**
Residence time (min)	X_1	5	10	15
Mass (g)	X_2	0.5	1.0	1.5

The original values were converted to log values, and the data were analyzed using a quadratic model to obtain the coefficients of the variables and to optimize the plasma treatment.

2.1. Drying Process

The drying process was monitored during the plasma treatment by intermittent sampling, with 5 samples by the end of each treatment. Mild (5 min-1.5 g), moderate (10 min-1.0 g), and extreme (15 min-0.5 g) conditions selected from bacterial inactivation were selected for evaluation of the drying process using plasma treatment in WF and WP. Wet and dry WF as well as wet and dry WP were tested for this purpose to assess the performance of plasma treatment and to select a model for prediction of the MR (moisture ratio) during dehydration. Four models including Page, 2-term exponential, Midilli and Henderson–Pabis were employed and fitted on the experimental data obtained for MR under each specific condition. The definition for MR and the four models used for the drying assessment are as follows:

$$MR = (M - M_e)/(M_0 - M_e)$$

Page model:

$$MR = \exp(-k \times t^n) \quad (1)$$

Two-term exponential model:

$$MR = a \times \exp(-k \times t) + (1 - a) \times \exp(-k \times a \times t); \quad (2)$$

Midilli model:

$$MR = a \times \exp(-k \times t^n) + b \times t; \quad (3)$$

Henderson–Pabis model:

$$MR = a \times \exp(-k \times t); \quad (4)$$

where M is the moisture content at time t, M_e is the equilibrium moisture content, and M_0 is the initial moisture content. Parameters a, b, k, and n are drying constants. To select the best model for prediction of the drying curve based on MR variation as the dependent variable versus time, the coefficient of determination (R^2), root mean square error (RMSE), and the trend of k values under different conditions of treatment for each material were compared and evaluated. RMSE can be described as the following equation:

$$RMSE = \sqrt{\frac{1}{N}\sum_{i=1}^{N}\left(MR_{pre} - MR_{exp}\right)^2} \quad (5)$$

where N is the number of observations, and MR_{pre} and MR_{exp} are the predicted (calculated by the model) and experimental values of MR.

2.2. Functional Properties

Functional properties including water absorption (for WF and WP), oil absorption (for WF and WP), protein solubility, and emulsifying activity index (EAI) (for WP) were determined as follows.

The water and oil absorption properties of untreated and treated WF and WP were determined following a method by Brishti et al. (2017) and Ratnawati et al. (2019) with some modifications [23,24]. An amount of 0.5 g of sample was mixed with 10 mL of distilled water or vegetable oil in a centrifuge tube. The mixture was mixed on a vortex mixer for 30 s and was given 15 min to stand at the lab temperature. Afterwards, it was centrifuged for 20 min at 3000 rpm, and the supernatant was decanted. The weight of the fluid absorbed by the sample was calculated and was divided by the original weight of the sample to determine the water or oil absorption capacity.

The solubility of whey protein in water was determined following an experimental method by Dissanayake et al. (2012) [25]. A 5% dispersion of protein in water was prepared, and after giving time for solubilization, it was centrifuged at 12,000× *g* at room temperature for 20 min. The percentage of solubility was determined by the nitrogen content in the supernatant (determined by Kjeldahl) converted to protein using the conversion factor of 6.38, which was finally divided by the original mass of the sample used for this test.

The emulsifying activity index was measured using a method proposed by Pearce and Kinsella (1978) and Cruz-Solorio (2018) [26,27]. In this method, 10 mL deionized water was added to 0.1 g of sample in powder form, and then 3.3 mL of canola oil was added to the suspension. The mixture was homogenized in a homogenizer for 1 min to prepare an emulsion. Thereafter, 50 µL of the emulsion was transferred in 5 mL sodium dodecyl sulfate (SDS: 0.1% concentration). Absorbance was measured at 500 nm in a 10 mm path length cuvette using a spectrophotometer. EAI (m^2/g) was determined as below:

$$EAI = (2 \times 2.3 \times A_0)/(0.25 \times W); \quad (6)$$

where A_0 is the absorbance and W (g) is the weight of the sample.

The color of the samples was measured using a color measurement machine (CM 2500d, Minolta Inc., Tokyo, Japan) in a three-coordinate system including L: lightness (black = 0, white = 100), a: greenness-redness (green = −a, red = +a), and b: blueness-yellowness (blue = −b, yellow = +b). The color change of the treated samples compared to the untreated material or reference was calculated as below (Soleimani et al., 2018) [28]:

$$\Delta E = [(\Delta L)^2 + (\Delta a)^2 + (\Delta b)^2]^{0.5}; \quad (7)$$

$$\text{Where } \Delta L = L_{treated} - L_{untreated}, \Delta a = a_{treated} - a_{untreated}, \text{ and } \Delta b = b_{treated} - b_{untreated}; \quad (8)$$

2.3. Data Analysis

Treatment of the materials was conducted following a central composite design (CCD-center faced) using the Design Expert software (ver. 10, Stat-Ease Inc., Minneapolis, MN, USA) with two factors for dry or wet WF and WP. Five replications were carried out at the center point of the design.

3. Results and Discussion

The results of the influence of cold plasma treatment on coliform inactivation in wheat flour and whey protein isolate are shown in Table 2 and the 3-D graphs in Figures 2 and 3. Plasma performance based on coliform Log reduction (in the unit mass of the substrate) was positively affected by residence time, but it was negatively affected by the sample weight in the reactor. Increasing time would provide more chance of incidence of the

reactive species in plasma with the bacteria in the substrate, which is the opposite of what was obtained for the increased weight of the sample in the reactor. Comparing the results of originally wet and dry WF indicates that better results in terms of bacterial inactivation could be obtained for the dry WF. A reason for this could be that water reactivity with the active species in plasma can protect microorganisms in the wet sample. For example, under a more severe condition (15 min-0.5 g) of treatment, a log reduction of over 4 was obtained with the dry sample. However, a maximal value of 3.4 was obtained with the wet sample.

Table 2. Coliform inactivation (log reduction) by combinations of plasma treatment parameters.

Combination	Parameter		Coliform Log Reduction			
	RT	Mass (g)	WFd	WFw	WPd	WPw
1	10	1.0	2.94	2.44	0.85	1.00
2	5	0.5	3.06	2.55	1.30	1.11
3	15	1.0	3.66	2.92	1.44	1.20
4	15	0.5	4.13	3.39	1.77	1.28
5	10	0.5	3.75	3.12	1.42	1.19
6	10	1.0	3.04	2.53	0.92	0.91
7	10	1.0	2.81	2.58	1.11	0.90
8	10	1.5	3.11	2.61	0.62	0.39
9	10	1.0	3.01	2.33	1.16	0.75
10	15	1.5	3.22	2.74	0.71	0.66
11	5	1.0	2.89	2.37	0.49	0.37
12	5	1.5	2.45	2.05	0.20	0.11
13	10	1.0	2.77	2.32	1.21	0.88

RT: residence time; WF_d: dry wheat flour (MC = 10%); WF_w: wet wheat flour (MC = 16%); WP_d: dry whey powder; WP_w: wet whey powder (MC = 16%).

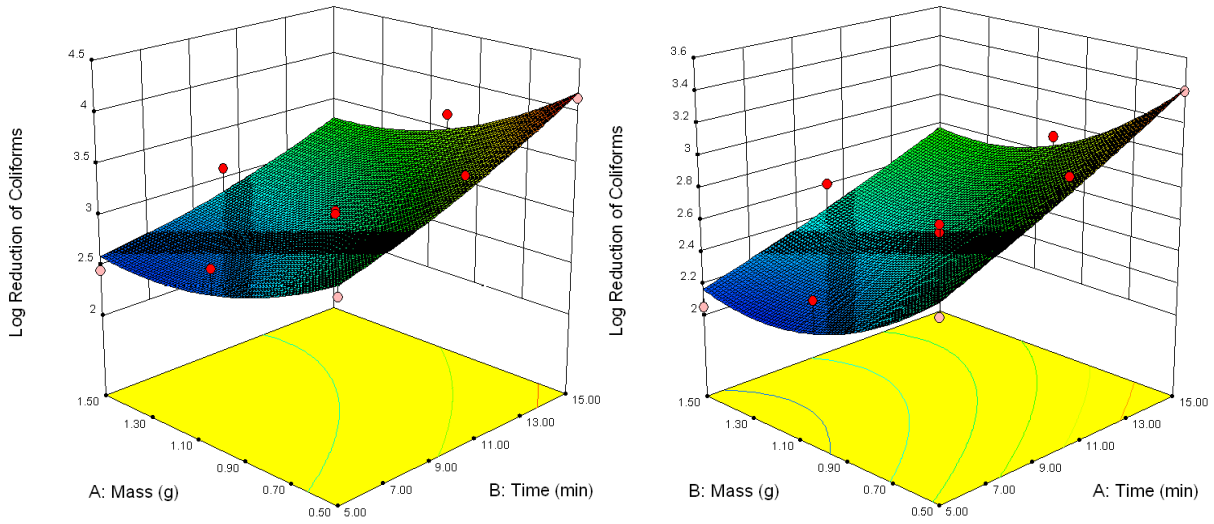

Figure 2. Response surface for coliform log reduction in WFd (**left**) and WFw (**right**) affected by plasma process parameters.

Similar results were obtained for WP such that log reductions of 1.3 and 1.7 were obtained for the wet and dry samples. Comparing the results for WF and WP indicates that plasma treatment is more effective on coliform inactivation in WF. This can be due to the more functional groups in protein (in WP) compared to the carbohydrates in WF, with more neutralization impact on the plasma gas species. Also, protein can play a nutritional/protective role for the bacteria against the harsh condition in the treatment that was applied. According to the results, if a log cycle reduction of 3 is the target in

the original sample, combinations of 1.4 g-12 min or 0.7 g-7 min and 0.8 g-15 min or 0.5 g-10 min for dry WF and wet WF would generate this outcome, respectively. However, this level of performance is not achievable for WP under such conditions. According to the optimization studies, maximal log reductions of 1.86 and 1.39 can be obtained for dry WP and wet WP, respectively, under the condition of 15 min-0.5 g. An extrapolation analysis using the parameters and verification of the results through an experimental study indicated that maximal log reductions of 2.2 and 1.3 are achievable for dry and wet WP under 26 min-0.3 g and 22 min-0.3 g, respectively. More severe conditions resulted in sample deterioration and a change in the appearance, according to the experimental results. Although successful results were obtained in this study on coliform bacterial inactivation in powder-form materials using plasma technology, very low log reductions have been reported by researchers. For example, Oh et al. (2015) reported that they could achieve up to 0.9 log reduction for *Cronobacter sakazakii* and 0.4 log reduction for *Bacillus cereus* in infant milk powder after plasma treatment using a high power (900 W) under vacuum [29]. Log reduction values of up to 2.1 and 1.9 were reported with high-power (900 W) plasma treatment for onion powder with *B. cereus* and *E. coli*, respectively.

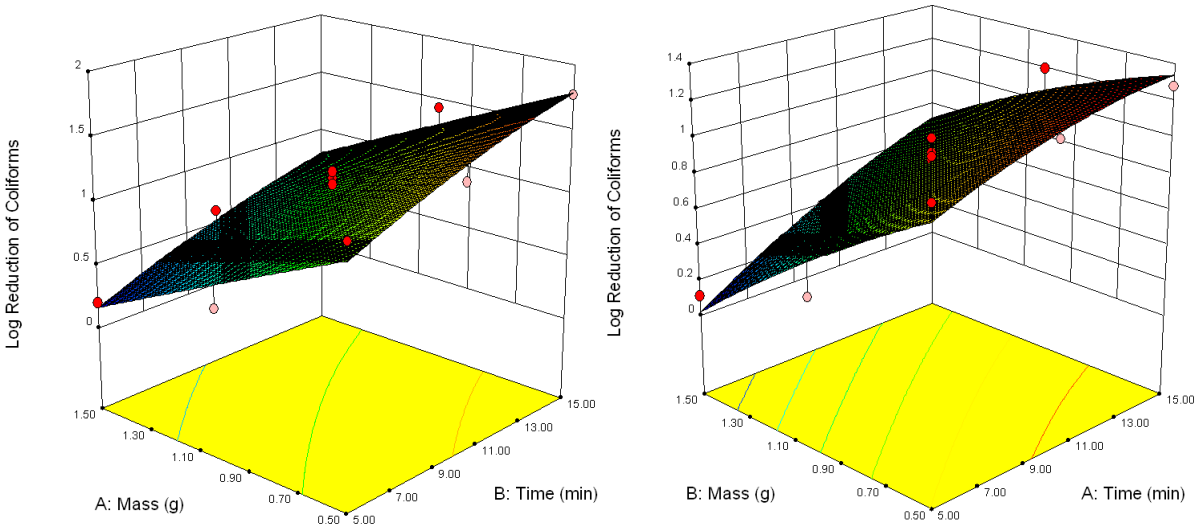

Figure 3. Response surface for coliform log reduction in WPd (**left**) and WPw (**right**) affected by plasma process parameters.

An optimization study employing a quadratic model resulted in the following equations for coliform inactivation in WF and WP. According to Table 3, the lack of fit of the models for dry and wet WF and WP was non-significant. According to the *p*-values obtained, time was the more effective factor compared to mass for dry and wet WP. However, for dry or wet WP, mass was the more effective factor in the process of coliform inactivation. The coefficients of process variables including time (x_1) and mass of the sample (x_2) in all models obtained were positive and negative, respectively.

$$\text{Dry WF: } \Delta = 3.83 + 0.05\ X_1 - 2.32\ x_2 - 0.03\ x_1\ x_2 + 0.003\ {x_1}^2 + 0.95\ {x_2}^2;\ r^2 = 0.88; \quad (9)$$

10 min-1 g results in: $\Delta = 2.96$
15 min-0.5 g results in: $\Delta = 4.11$

$$\text{Wet WF: } \Delta = 3.24 + 0.07\ X_1 - 2.49\ x_2 - 0.001\ x_1\ x_2 + 0.0002\ {x_1}^2 + 0.97\ {x_2}^2;\ r^2 = 0.89; \quad (10)$$

10 min-1 g results in: $\Delta = 2.43$

15 min-0.5 g results in: $\Delta = 3.32$

$$\text{Dry WP: } \Delta = 1.17 + 0.10\,X_1 - 0.95\,x_2 + 0.003\,x_1\,x_2 - 0.002\,{x_1}^2 - 0.03\,{x_2}^2;\ r^2 = 0.91; \quad (11)$$

10 min-1 g results in: $\Delta = 1.02$
15 min-0.5 g results in: $\Delta = 1.76$

$$\text{Wet WP: } \Delta = 1.11 + 0.06\,X_1 - 0.81\,x_2 + 0.037\,x_1\,x_2 - 0.002\,{x_1}^2 - 0.18\,{x_2}^2;\ r^2 = 0.93; \quad (12)$$

10 min-1 g results in: $\Delta = 0.89$
15 min-0.5 g results in: $\Delta = 1.39$
Where Δ is log reduction, and x_1 and x_2 are residence time and sample mass.

Table 3. Analysis of variance (ANOVA) for log cycle reduction in coliform bacteria in WF and WP using air (0.2 L/min) as the carrier gas.

Source	df	Dry WF		Wet WF		Dry WP		Wet WP	
		MSE	*p* Value	MSE	*p* Value	MSE	*p* Value	MSE	*p* Value
Model	5	0.44	0.0040	0.46	0.0001	0.42	0.0015	0.29	0.0007
X_1	1	1.14	0.0013	0.73	0.0002	0.61	0.0025	0.41	0.0015
X_2	1	0.78	0.0037	0.45	0.0010	1.45	0.0002	0.97	0.0001
$X_1.X_2$	1	0.022	0.4911	0.020	0.5998	0.0002	0.9325	0.034	0.1849
${X_1}^2$	1	0.019	0.5258	0.021	0.8056	0.007	0.6259	0.010	0.4515
${X_2}^2$	1	0.16	0.0970	0.19	0.0126	0.0001	0.9445	0.006	0.5680
Residual	7	0.043		0.020		0.029		0.016	
Lack of fit	3	0.080	0.0646 ^{NS}	0.025	0.2895 ^{NS}	0.035	0.3555 ^{NS}	0.026	0.1471 ^{NS}
Error	4	0.014		0.014		0.25		0.008	
Corrected total	12								

X_1: time (min); X_2: mass (g) of sample; NS: not significant.

The chemical compositions of the untreated and plasma-treated WF and WP are presented in Table 4. The results indicate that the chemical composition of the materials in terms of protein content, crude fiber, dietary fiber, starch and ash would not significantly change with ACP treatment.

Table 4. Chemical composition of untreated and plasma-treated WF and WP.

Material	CP (db)	CF (db)	DF (db)	Starch (db)	Ash (db)
UWF	14.8	1.22	2.66	74.9	0.47
UWP	90.2	0.30	0	0	5.7
TWF	14.9	1.09	2.59	74.6	0.44
TWP	90.3	0.33	0	0	5.9

CP: crude protein, CF: crude fat, DF: dietary fiber, UWFl: untreated wheat flour, UWP: untreated whey protein.

The drying parameters of the models employed to describe the dehydration of WF and WP are presented in Tables 5–8.

Table 5. Parameters of different models for WFd drying during plasma treatment using 0.2 L/min air flowrate.

Combination	Model	DF	Parameters	R^2	RMSE
5 min-1.5 g	Page	2	k = 0.132, n = 0.652	0.994	0.019
	2-term	1	a = 0.118, k = 0.438	0.998	0.025
	Midilli	4	a = 1.528, b = 0.018, k = 0.464, n = 0.469	0.0.995	0.215
	Henderson and Pabis	2	a = 0.961, k = 0.062	0.997	0.036
10 min-1.0 g	Page	2	k = 0.200, n = 0.989	0.999	0.019
	2-term	1	a = 0.678, k = 0.136	0.999	0.025
	Midilli	4	a = 0.797, b = 0.024, k = 0.024, n = 2.009	0.999	0.215
	Henderson and Pabis	2	a = 0.997, k = 0.120	0.999	0.036
15 min-0.5 g	Page	2	k = 0.132, n = 1,141	0.994	0.031
	2-term	1	a = 0.999, k = 0.169	0.996	0.036
	Midilli	4	a = 0.720, b = 0.009, k = 0.010, n = 2.410	0.999	0.114
	Henderson and Pabis	2	a = 1.010, k = 0.171	0.996	0.037

Table 6. Parameters of different models for WFw drying during plasma treatment using 0.2 L/min air flowrate.

Combination	Model	DF	Parameters	R^2	RMSE
5 min-1.5 g	Page	2	k = 0.056, n = 0.986	0.999	0.015
	2-term	1	a = 0.998, k = 0.055	0.999	0.015
	Midilli	4	a = 0.960, b = −0.039, k = 0, n = 1.000	0.999	0.019
	Henderson and Pabis	2	a = 0.995, k = 0.054	0.999	0.014
10 min-1.0 g	Page	2	k = 0.089, n = 1.057	0.997	0.034
	2-term	1	a = 0.357, k = 0.178	0.998	0.028
	Midilli	4	a = 0.813, b = 0.040, k = 0.019, n = 2.202	0.999	0.078
	Henderson and Pabis	2	a = 0.995, k = 0.094	0.998	0.029
15 mni-0.5 g	Page	2	k = 0.175, n = 0.853	0.999	0.015
	2-term	1	a = 0.737, k = 0.147	0.998	0.025
	Midilli	4	a = 0.824, b = −0.022, k = 0.051, n = 1.027	0.994	0.079
	Henderson and Pabis	2	a = 0.982, k = 0.132	0.999	0.024

Table 7. Parameters of different models for WPd drying during plasma treatment using 0.2 L/min air flowrate.

Combination	Model	DF	Parameters	R^2	RMSE
5 min-1.5 g	Page	2	k = 0.094, n = 0.590	0.999	0.014
	2-term	1	a = 0.092, k = 0.301	0.999	0.026
	Midilli	4	a = 1.013, b = 0.021, k = 0.090, n = 0.929	0.999	0.001
	Henderson and Pabis	2	a = 0.957, k = 0.031	0.998	0.034
10 min-1.0 g	Page	2	k = 0.133, n = 0.755	0.998	0.022
	2-term	1	a = 0.141, k = 0.448	0.999	0.023
	Midilli	4	a = 1.000, b = −0.040, k = 0.148, n = 0.010	0.997	0.033
	Henderson and Pabis	2	a = 0.971, k = 0.079	0.997	0.033
15 min-0.5 g	Page	2	k = 0.105, n = 0.979	0.997	0.026
	2-term	1	a = 0.523, k = 0.136	0.998	0.025
	Midilli	4	a = 0.777, b = 0.016, k = 0.011, n = 2.160	0.999	0.092
	Henderson and Pabis	2	a = 0.999, k = 0.100	0.999	0.026

Table 8. Parameters of different models for WPw drying during plasma treatment using 0.2 L/min air flowrate.

Combination	Model	DF	Parameters	R^2	RMSE
5 min-1.5 g	Page	2	k = 0.116, n = 0.561	0.999	0.018
	2-term	1	a = 0.087, k = 0.430	0.999	0.030
	Midilli	4	a = 1.275, b = 0.027, k = 0.300, n = 0.577	0.999	0.152
	Henderson and Pabis	2	a = 0.957, k = 0.042	0.998	0.037
10-min1.0 g	Page	2	k = 0.081, n = 0.961	0.999	0.021
	2-term	1	a = 0.387, k = 0.128	0.999	0.020
	Midilli	4	a = 1.373, b = −0.011, k = 0.328, n = 0.407	0.999	0.154
	Henderson and Pabis	2	a = 0.997, k = 0.075	0.999	0.020
15 min-0.5 g	Page	2	k = 0.151, n = 0.810	0.997	0.030
	2-term	1	a = 0.677, k = 0.119	0.994	0.038
	Midilli	4	a = 0.790, b = 0.018, k = 0.033, n = 1.637	0.997	0.090
	Henderson and Pabis	2	a = 0.971, k = 0.101	0.997	0.035

High values of the coefficient of determination and RMSE indicated that all four models can be used to estimate the MC of both materials during plasma treatment. Among all models, the Henderson–Pabis model was found to be a more applicable model. The higher suitability of this model is due to three reasons: (1) the simplicity of model, (2) the low deviation between the estimated values and the experimental data points during drying, and (3) the reasonable drying constant (k), with a proper trend obtained by the process severity such that by increasing the severity, the values of k increased while the

value of accessible water for evaporation (a) was almost constant (≈1.0). As an example, the values of k using the Henderson–Pabis model for dry WF (WFd: with 10% original MC) under conditions of 5 min-1.5 g, 10 min-1 g, and 15 min-0.5 g (with an increased level of process severity) were 0.062, 0.120, and 0.171 (Table 5). This is an indication of an accelerated drying process due to the smaller sample size. In other words, although the residence time would increase, leading to a lower slope towards the end of the process, the overall k would increase, which is the consequence of having a higher ratio of plasma power to the size of the sample.

A similar increasing trend of k values was obtained for wet WF as well as dry or wet WP with reduced size of samples. Comparing WF with WP, lower drying rates were achieved for WP. For example, k values of 0.031, 0.079, and 0.100 were obtained for combinations of 5 min-1.5 g, 10 min-1 g, and 15 min-0.5 g in WPd (Table 7).

The lower drying rate constant values for WP under a similar combination of parameters compared to those of WF show that WP is more resistant to moisture loss, which could be due to the higher hydrophilicity of the latter material. In other words, the presence of a large number of a wide variety of hydrophilic groups such as amine, amide, carboxyl, and hydroxyl would be a reason for a slower water loss in WP compared with WF, with hydroxyl as the major hydrophilic group located on starch macromolecules.

Altogether, it can be concluded that ACP can be used as a fast-drying approach for dehydration of food or nutraceuticals to low levels of MC. In a study conducted by Shishir et al. (2019), it was reported that cold plasma can be used as an effective pre-treatment to accelerate the drying process of shiitake mushrooms due to surface topography improvement, resulting in enhanced mass transfer during dehydration [21]. In another study by Bao et al. (2021), an accelerated drying process was reported in jujube slices using cold plasma pre-treatment, with a high antioxidant capacity in the dried product [22]. A drying effect of low-temperature plasma treatment on basmati rice and granular starch was reported by Thirumdas et al. (2015) and Lii et al. (2002), respectively [30,31]. The main reason for the fast drying impact of plasma in this study can be the dry air used as the carrier gas in the process, although Sarangapani et al. (2015, 2017) reported that moisture loss can be mainly due to water decomposition and conversion to the active species removed from the system by the vacuum [32,33]. The drying curve for WF under three conditions following the experimental results and data obtained using the Henderson–Pabis model are presented in Figure 4.

Composition analysis indicated that the main components such as protein, carbohydrates, and fiber did not change with plasma treatment in this study. A similar result was reported by Chen et al. (2012) and Thirumdas et al. (2016) [34,35]. However, Deng et al. (2007), who worked on plasma treatment of black gram, concluded that there could be some variations in the protein content. The functional properties (water absorption, oil absorption, protein solubility, and emulsifying activity index), bulk density, and color of the samples are presented in Table 9.

According to the results presented in Table 9, water absorption increased with plasma treatment in WF from 104.5% in untreated material to 118.3% (in lightly treated sample: WF(5 min-1.5 g)), 174.4% (in medium-treated sample: WF(10 min-1.0 g)) and 180.9% (in severely treated sample: WF(15 min-0.5 g)). A higher water absorption capacity was also reported by Sarangapani et al. (2017) in black gram and Sarangapani et al. (2015) in parboiled rice after plasma treatment [32,33]. This increased water absorption can be due to the generation of larger voids in the bulk of the sample after treatment, trapping more water in the bulk of material. In other words, and as the SEM imaging (Figure 5) shows, by increasing the plasma treatment intensity (the ratio of plasma power to sample size), larger particles were generated (due to clustering of microparticles—clustering could

be due to partial ionization of some of the groups in the molecules and the attraction of some molecules with an opposite charge, generating larger particles as a result). Another reason could be collision of the particles and molecules and generation of static electricity, as well as the presence of water in the materials, which improves the hydrogen bonding between the molecules and the particles as a result. The maximum particle size in the untreated WF was 150 µm and reached approximately 200 µm in the treated samples. At the same time, the ratio of larger particles to smaller particles increased with process intensity, resulting in higher voids in the samples treated under more severe conditions. SEM and bulk density are proof of this phenomenon of void increases in the treated samples, with more significance in the ones treated under more severe conditions (WF(15 min-0.5 g)). The bulk density was reduced by plasma treatment from 610 kg/m^3 in untreated WF to less than 577 kg/m^3 in the treated WFs. This means that a higher volume of voids has been generated by plasma treatment in most of the samples.

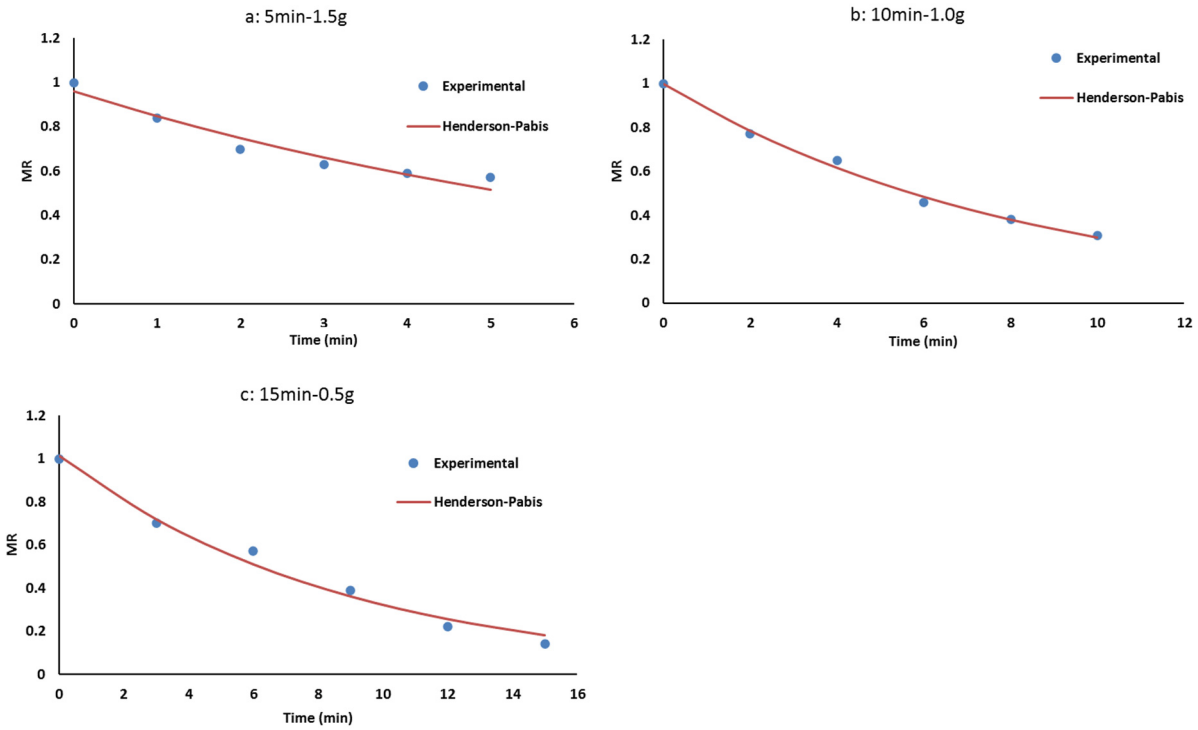

Figure 4. Experimental and predicted (Henderson–Pabis) drying curves for dry WF (10% MC) under different conditions; (**a**): 5 min-1.5 g; (**b**): 10 min-1.0 g; (**c**): 15 min-0.5 g.

Table 9. Functional and physical properties of untreated and plasma-treated WF and WP.

Material	WA (%)	OA (%)	PS (%)	EAI (m^2/g)	BD (kg/m^3)	L	a	b	ΔL
WF	104.5	176.5	NA	NA	610	90.74	0.60	8.24	0.00
WF (5–1.5)	118.3	183.5	NA	NA	577	89.62	0.41	7.62	1.29
WF (10–1.0)	174.4	183.9	NA	NA	560	89.26	0.13	7.46	1.73
WF (15–0.5)	180.9	184.7	NA	NA	556	87.10	0.09	7.39	3.77
WP	NA	231.9	96.5	22.04	407	92.69	−0.03	11.53	0.00
WP (5–1.5)	NA	240.5	93.6	23.60	390	91.81	−0.05	11.72	0.90
WP (10–1.0)	NA	246.9	93.1	24.58	380	91.57	−0.04	11.22	1.16
WP (15–0.5)	NA	253.0	93.9	24.33	385	91.11	0.07	13.53	2.55

WA: water absorption; OA: oil absorption; PS: protein solubility; EAI: emulsifying activity index, BD: bulk density; WF: wheat flour; WP: whey protein. NA: not applicable.

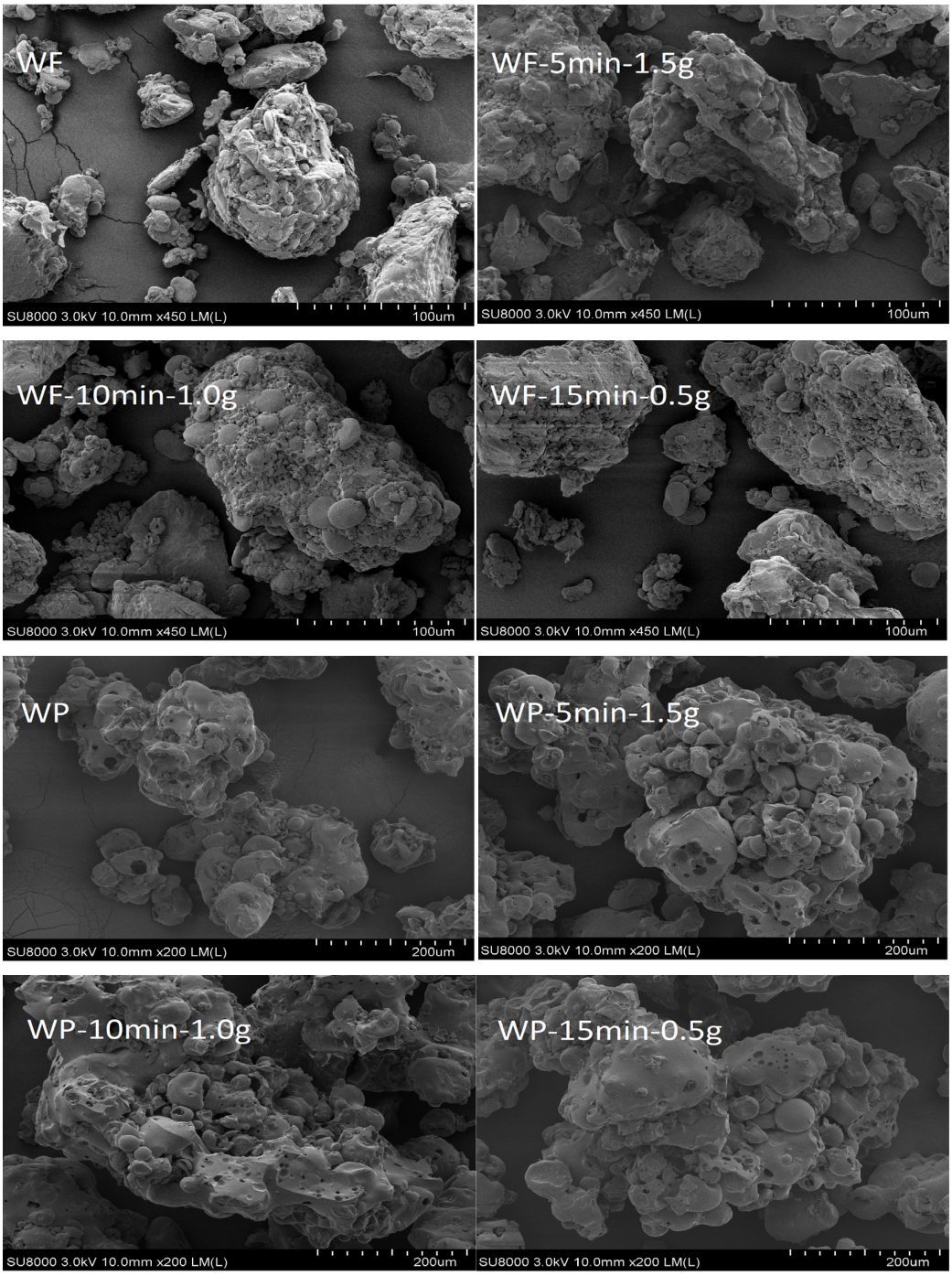

Figure 5. Scanning electron microscopy (SEM) of untreated and treated WF and WP; WF: wheat flour; WP: whey protein.

In WP, water absorption was not measurable due to the fast solubility of this material in water.

Oil absorption was measured in both WF and WP, which in average was much higher in WP or treated WP compared with WF or treated WF. For example, oil absorption in untreated WF was 176.5%, which was much less than that obtained for the untreated WP of 231.9% oil absorption (Table 9). This means that untreated WP showed a 31% higher oil absorption compared to untreated WF. The main reason for this higher oil absorption in WP is a higher particle size or voids. The maximum particle size in untreated WP was 250 μm compared to 150 μm in untreated WF, as seen in the SEM imaging. This is reflected in the bulk density values, as a value of 407 kg/m^3 was obtained for untreated WP compared to

610 kg/m^3 obtained for untreated WF (Table 9). The particle size of the treated WPs showed a significant enlargement (to about 600 μm) due to the clustering of the particles. As a result, a similar increasing trend was obtained for WF and WP with the plasma treatment.

However, the impact of plasma treatment on oil absorption improvement was much lower than its impact on water absorption elevation, such that only approximately a 5% increase in oil absorption was obtained for WF or WP by plasma treatment (Table 9). Oil absorption was slightly affected by the treatment severity in both materials.

The results of protein solubility measurements in WP indicated that it was slightly affected by plasma treatment, with approximately a 3% reduction (Table 9). This minor reduction in solubility can be because of minor surface charge modification or denaturation, which need more studies. The emulsifying activity index (EAI) was slightly increased by plasma treatment with approximately up to 11% in WP(10 min-1.0 g).

The color change in the treated materials was not visually noticeable. However, after analyzing by the Minolta color analyzer, a minor change was observed by plasma treatment such that a slightly lower value of L was observed in the treated WF and WP compared to the untreated materials (Table 9). The overall color change (ΔL) values indicated that this parameter would be slightly affected/increased by the severity of the treatment such that by reducing the sample mass in the reactor, increased values of ΔL were observed with up to 3.77 in WF (15–0.5 g) and 2.55 in WP (15–0.5 g). The low values of color change show that plasma treatment would not adversely modify the appearance of the products and would retain this important quality attribute. Other studies also showed low or no change in the appearance and color of the products treated by plasma at different operation conditions (Misra et al., 2014, 2015; Kovacevic et al., 2016; Ramazzina et al., 2015; Mahendran 2016; Ziuzina et al., 2016; Kim et al., 2017; Oh et al., 2017; Trevisani et al., 2017; Pankaj et al., 2018) [12,36–44].

4. Conclusions

The results of this study indicated that cold plasma treatment can be used as an effective process for inactivation of coliform bacteria in powder-form materials. However, its performance depends on process conditions as well as the type of material. Similar conditions in this study resulted in much better inactivation results in a starch carbohydrate-rich material such as wheat flour compared with a protein-rich material as whey protein. According to the results, in the range studied, a maximum inactivation (log reduction) of 4.13 and 1.77 was obtained for WF and WP, respectively. A drying kinetics study indicated that ACP treatment can be used as a fast-drying method for powder-form material dehydration with almost no change in the quantity of the major components in a carbohydrate- or protein-based material. The lower bulk density of the materials that underwent the ACP treatment could be due to the size enlargement of the particles after treatment. In terms of functional properties, other than water absorption in WF which was highly affected by ACP treatment (by 80% enhancement), the rest of the functional properties were slightly affected.

Author Contributions: M.S.: proposal writing, funding application, draft writing, development and preparation, experimental design, data collection and analysis. O.-D.B.: project administration, proposal writing, funding application, contribution in experimental design, lab and facilities provision, writing/review and editing the manuscript. All authors have read and agreed to the published version of the manuscript.

Funding: This research received funding from Saskatchewan ADF (#20180293).

Data Availability Statement: Data are contained within the article.

Acknowledgments: The authors would like to acknowledge the Department of Chemical and Biological Engineering, University of Saskatchewan, for all the support during this study. The authors also would like to acknowledge Saskatchewan ADF for supporting this project financially.

Conflicts of Interest: The authors declare no conflicts of interest.

References

1. Awuah, G.B.; Ramaswamy, H.S.; Economides, A. Thermal processing and quality: Principles and overview. *Chem. Eng. Prog.* **2007**, *46*, 584–602. [CrossRef]
2. Lou, X.; Jin, Y.; Tian, H.; Yu, H.; Chen, C.; Hanna, M.; Lin, Y.; Yuan, L.; Wang, J.; Xu, H. High-pressure and thermal processing of cloudy hawthorn berry (*Crataegus pinnatifida*) juice: Impact on microbial shelf-life, enzyme activity and quality-related attributes. *Food Chem.* **2022**, *372*, 131313. [CrossRef]
3. Allai, F.M.; Azad, Z.R.A.; Mir, N.A.; Gul, K. Recent advances in non-thermal processing technologies for enhancing shelf life and improving food safety. *Appl. Food Res.* **2023**, *3*, 100258. [CrossRef]
4. Leong, S.Y.; Duque, S.M.M.; Conde, L.A.; Khrisanapant, P.; Oey, I. Addressing the opportunities of non-thermal food processing technologies in the ASEAN region context. *Int. J. Food Sci. Technol.* **2024**, *59*, 7739–7753. [CrossRef]
5. Maccaferri, C.; Gherardi, M.; Laurita, R. Evaluating atmospheric pressure cold plasma decontamination techniques for packaging materials: A systematic review and meta-analysis. *Front. Phys.* **2024**, *12*, 1399720. [CrossRef]
6. Pasdar, N.; Mostashari, P.; Greiner, R.; Khelfa, A.; Rashidinejad, A.; Eshpari, H.; Vale, J.M.; Gharibzahedi, S.M.T.; Roohinejad, S. Advancements in non-thermal processing technologies for enhancing safety and quality of infant and baby food products: A review. *Foods* **2024**, *13*, 2659. [CrossRef]
7. Lopez, M.; Calvo, T.; Prieto, M.; Mugica-Vidal, R.; Muro-Fraguas, I.; Alba-Elias, F.; Alvarez-Ordonez, A. A review on non-thermal atmospheric plasma for food preservation: Mode of action, determinants of effectiveness, and applications. *Front. Microbiol.* **2019**, *10*, 622. [CrossRef]
8. Tabares, F.L. *Plasma Applications for Material Modification: From Microelectronics to Biological Materials*, 1st ed.; Jenny Stanford Publishing: Singapore, 2021; p. 322.
9. Tabares, F.L.; Junkar, I. Cold plasma systems and their application in surface treatments for medicine. *Molecules* **2021**, *26*, 1903. [CrossRef] [PubMed]
10. Ouyang, B.; Zhang, Y.; Xia, X.; Rawat, R.S.; Fan, H.J. A brief review on plasma for synthesis and processing of electrode materials. *Mater. Today Nano* **2018**, *3*, 28–47. [CrossRef]
11. Daeschlein, G.; von Woedtke, T.; Kindel, E.; Brandenburg, R.; Weltmann, K.-D.; Jünger, M. Antibacterial activity of an atmospheric pressure plasma jet against relevant wound pathogens in vitro on a simulated wound environment. *Plasma Process Polym.* **2010**, *7*, 224–230. [CrossRef]
12. Pankaj, S.K.; Wan, Z.; Keener, K.M. Effect of cold plasma on food quality: A review. *Foods* **2018**, *7*, 4. [CrossRef]
13. Wolf, R.A. *Atmospheric Pressure Plasma for Surface Modification*, 1st ed.; Wiley: Hoboken, NJ, USA, 2012; p. 264. [CrossRef]
14. Klämpfl, T.G.; Isbary, G.; Shimizu, T.; Li, Y.F.; Zimmermann, J.L.; Stolz, W.; Schlegel, J.; Morfill, G.E.; Schmidt, H.-U. Cold atmospheric air plasma sterilization against spores and other microorganisms of clinical interest. *Appl. Environ. Microbiol.* **2012**, *78*, 5077–5082. [CrossRef]
15. Tseng, S.; Abramzon, N.; Jackson, J.O.; Lin, W.-J. Gas discharge plasmas are effective in inactivating Bacillus and Clostridium spores. *Appl. Microbiol. Biotechnol.* **2012**, *93*, 2563–2570. [CrossRef]
16. Deng, S.; Ruan, R.; Mok, C.K.; Huang, G.; Lin, X.; Chen, P. Inactivation of *Escherichia coli* on almonds using nonthermal plasma. *J. Food Sci.* **2007**, *72*, 62–66. [CrossRef] [PubMed]
17. Lassen, K.S.; Nordby, B.; Grun, R. The dependence of the sporicidal effects on the power and pressure of RF-generated plasma processes. *J. Biomed. Mater. Res. Part B Appl. Biomater.* **2005**, *7*, 553–559. [CrossRef]
18. Han, L.; Patil, S.; Boehm, D.; Milosavljevic, V.; Cullen, P.J.; Bourkea, P. Mechanisms of inactivation by high-voltage atmospheric cold plasma differ for *Escherichia coli* and *Staphylococcus aureus*. *Appl. Environ. Microbiol.* **2016**, *82*, 450–458. [CrossRef] [PubMed]
19. Traba, C.; Liang, J.F. The inactivation of *Staphylococcus aureus* biofilms using low-power argon plasma in a layer-by-layer approach. *Biofouling* **2015**, *31*, 39–48. [CrossRef]
20. Li, S.; Chen, S.; Han, F.; Xv, Y.; Sun, H.; Ma, Z.; Chen, J.; Wu, W. Development and Optimization of Cold Plasma Pretreatment for Drying on Corn Kernels. *J. Food Sci.* **2019**, *84*, 2181–2189. [CrossRef]
21. Shishir, M.R.I.; Karim, N.; Bao, T.; Gowd, V.; Ding, T.; Sun, C. Cold plasma pretreatment—A novel approach to improve the hot air drying characteristics, kinetic parameters, and nutritional attributes of shiitake mushroom. *Dry. Technol.* **2020**, *38*, 2134–2150. [CrossRef]
22. Bao, T.; Hao, X.; Shishir, M.R.; Karim, N.; Chen, W. Green alternative methods for pretreatment of whole jujube before the drying process. *J. Sci. Food Aric.* **2021**, *102*, 1030–1039. [CrossRef] [PubMed]

23. Brishti, F.H.; Zarei, M.; Muhammad, S.K.S.; Ismail-Futry, M.R.; Shukri, R.; Saari, N. Evaluation of the functional properties of mung bean protein isolate for development of textured vegetable protein. *Int. Food Res. J.* **2017**, *24*, 1595–1605.
24. Ratnawati, L.; Desnilasari, D.; Surahman, D.N.; Kumalasari, R. Evaluation of physicochemical, functional and pasting properties of soybean, mung bean and red kidney bean flour as ingredient in biscuit. In Proceedings of the IOP Conference Series: Earth and Environmental Science, Orlando, FL, USA, 1 November 2019. [CrossRef]
25. Dissanayake, M.; Liyanaarachchi, S.; Vasiljevic, T. Functional properties of whey proteins microparticulated at low pH. *J. Dairy Sci.* **2012**, *95*, 1667–1679. [CrossRef]
26. Pearce, K.N.; Kinsella, J.E. Emulsifying properties of proteins: Evaluation of a turbidimetric technique. *J. Agric. Food Chem.* **1978**, *26*, 716–723. [CrossRef]
27. Cruz-Solorio, A. Villanueva-Arce, R.; Garín-Aguilar, M.E.; Leal-Lara, H.; Toro, G.V. Functional properties of flours and protein concentrates of 3 strains of the edible mushroom *Pleurotus ostreatus*. *J. Food Sci. Technol.* **2018**, *55*, 3892–3901. [CrossRef] [PubMed]
28. Soleimani, M.; Tabil, L.G.; Oguocha, I.; Fung, J. Interactive influence of biofiber composition and elastomer on physico-mechanical properties of PLA green composites. *J. Environ. Polym. Degrad.* **2018**, *26*, 532–542. [CrossRef]
29. Oh, Y.J.; Lee, H.; Kim, J.E.; Lee, S.H. Cold Plasma Treatment Application to Improve Microbiological Safety of Infant Milk Powder and Onion Powder. *Korean J. Food Sci. Technol.* **2015**, *47*, 486–491. [CrossRef]
30. Thirumdas, R.; Deshmukh, R.; Annapure, U. Effect of low temperature plasma processing on physicochemical properties and cooking quality of basmati rice. *Innov. Food Sci. Emerg. Technol.* **2015**, *31*, 83–90. [CrossRef]
31. Lii, C.; Liao, C.; Stobinski, L.; Tomasik, P. Behaviour of granular starches in low-pressure glow plasma. *Carbohydr. Polym.* **2002**, *49*, 499–507. [CrossRef]
32. Sarangapani, C.; Devi, Y.; Thirumdas, R.; Annapure, U.S.; Deshmukh, R.R. Effect of low-pressure plasma on physico-chemical properties of parboiled rice. *Food Sci. Technol.* **2015**, *63*, 452–460. [CrossRef]
33. Sarangapani, C.; Devi, Y.; Thirumdas, R.; Trimukhe, A.; Deshmukh, R.R.; Annapure, U.S. Physico-chemical properties of low-pressure plasma treated black gram. *Food Sci. Technol.* **2017**, *79*, 102–110. [CrossRef]
34. Chen, H.H.; Chen, Y.K.; Chang, H.C. Evaluation of physicochemical properties of plasma treated brown rice. *Food Chem.* **2012**, *135*, 74–79. [CrossRef]
35. Thirumdas, R.; Saragapani, C.; Ajinkya, M.T.; Deshmukh, R.R.; Annapure, U.S. Influence of low-pressure cold plasma on cooking and textural properties of brown rice. *Innov. Food Sci. Emerg. Technol.* **2016**, *37*, 53–60. [CrossRef]
36. Misra, N.; Patil, S.; Moiseev, T.; Bourke, P.; Mosnier, J.; Keener, K.; Cullen, P. In-package atmospheric pressure cold plasma treatment of strawberries. *J. Food Eng.* **2014**, *125*, 131–138. [CrossRef]
37. Misra, N.N.; Kaur, S.; Tiwari, B.K.; Kaur, A.; Singh, N.; Cullen, P.J. Atmospheric pressure cold plasma (ACP) treatment of wheat flour. *Food Hydrocoll.* **2015**, *44*, 115–121. [CrossRef]
38. Kovacevic, D.B.; Putnik, P.; Dragovic-Uzelac, V.; Pedisic, S.; Jambrak, A.R.; Herceg, Z. Effects of cold atmospheric gas phase plasma on anthocyanins and color in pomegranate juice. *Food Chem.* **2016**, *190*, 317–323. [CrossRef]
39. Ramazzina, I.; Berardinelli, A.; Rizzi, F.; Tappi, S.; Ragni, L.; Sacchetti, G.; Rocculi, P. Effect of cold plasma treatment on physico-chemical parameters and antioxidant activity of minimally processed kiwifruit. *Postharvest Biol. Technol.* **2015**, *107*, 55–65. [CrossRef]
40. Mahendran, R. Effect of cold plasma on mortality of *Tribolium castaneum* on refined wheat flour. In Proceedings of the 10th International Conference on Controlled Atmosphere and Fumigation in Stored Products, Winnipeg, MB, Canada, 7–11 November 2016; pp. 142–146.
41. Ziuzina, D.; Misra, N.; Cullen, P.; Keener, K.; Mosnier, J.; Vilaro, I.; Gaston, E.; Bourke, P. Demonstrating the potential of industrial scale in-package atmospheric cold plasma for decontamination of cherry tomatoes. *Plasma Med.* **2016**, *6*, 397–412. [CrossRef]
42. Kim, J.E.; Oh, Y.J.; Won, M.Y.; Lee, K.S.; Min, S.C. Microbial decontamination of onion powder using microwave-powered cold plasma treatments. *Food Microbiol.* **2017**, *62*, 112–123. [CrossRef] [PubMed]
43. Oh, Y.J.; Song, A.Y.; Min, S.C. Inhibition of Salmonella typhimurium on radish sprouts using nitrogen-cold plasma. *Int. J. Food Microbiol.* **2017**, *49*, 66–71. [CrossRef] [PubMed]
44. Trevisani, M.; Berardinelli, A.; Cevoli, C.; Cecchini, M.; Ragni, L.; Pasquali, F. Effects of sanitizing treatments with atmospheric cold plasma, SDS and lactic acid on verotoxin-producing Escherichia coli and *Listeria monocytogenes* in red chicory (radicchio). *Food Control* **2017**, *78*, 138–143. [CrossRef]

Disclaimer/Publisher's Note: The statements, opinions and data contained in all publications are solely those of the individual author(s) and contributor(s) and not of MDPI and/or the editor(s). MDPI and/or the editor(s) disclaim responsibility for any injury to people or property resulting from any ideas, methods, instructions or products referred to in the content.